



Proceedings of the

15th *International Conference
on CAD/CAM Robotics & Factories
of the Future CARS & FOF99*

August, 18-20, 1999

Águas de Lindóia - Brazil

Volume 2

CHAOTIC PHENOMENA IN THE TRAJECTORY CONTROL OF REDUNDANT MANIPULATORS

Fernando B. M. Duarte
Escola Superior de Tecnologia Viseu
Dep. Matemática, Campus Politécnico
3510 Viseu, Portugal
 Tel: +351-32-480500, Fax: +351-32-424651
 Email: fduarte@mat.estv.ipv.pt

J. A. Tenreiro Machado
Instituto Politécnico do Porto
Instituto Superior de Engenharia
Departamento de Engenharia Electrotécnica
Rua de S. Tomé, 4200 Porto, Portugal
 Email: jtm@dee.isep.ipp.pt

Abstract - Redundant manipulators have some advantages when compared with classical arms because they allow the trajectory optimization, both on the free space and on the presence of obstacles, and the resolution of singularities. For this type of manipulators, the proposed kinematic control algorithms adopt generalized inverse matrices. In this line of thought, the generalized inverse control scheme is tested through several experiments that reveal the difficulties that often arise. Motivated by these problems this paper studies the chaos revealed by the kinematics trajectory planning scheme, as well as its influence on the dynamics, when controlling redundant and hyper-redundant manipulators. The results reveal several fundamental properties of the chaotic phenomena and gives a deeper insight towards the future development of superior trajectory control algorithms.

I. INTRODUCTION

A kinematically redundant manipulator is a robotic arm possessing more degrees of freedom (*dof*) than those required to establish an arbitrary position and orientation of the end effector. Redundant manipulators offer several potential advantages over non-redundant arms. In a workspace with obstacles, the extra degrees of freedom can be used to move around or between obstacles and thereby to manipulate in situations that otherwise would be inaccessible [1, 2, 4].

When a manipulator is redundant, it is anticipated that the inverse kinematics admits an infinite number of solutions. This implies that, for a given location of the manipulator's end effector, it is possible to induce a self-motion of the structure without changing the location of the gripper. Thus, the arm can be reconfigured to find better postures for an assigned set of task requirements.

Most of the techniques for solving the kinematics of redundant manipulators that have been suggested control the end effector indirectly, through the rates at which the joints are driven, using the pseudoinverse of the Jacobian [3]. Nevertheless, these algorithms lead to a kind of chaotic motion with unpredictable arm configurations. Therefore, an important area of research remains open and more efficient algorithms must be envisaged [5, 6, 7].

Having these ideas in mind, the paper is organized as follows. Section 2 introduces the formalism for the kinematics of redundant manipulators. Based on these concepts, section 3 presents several experiments with the kinematics and dynamics of different redundant robots. The results reveal a chaotic behavior that is further analyzed in section 4. Finally, section 5 draws the main conclusions.

II. KINEMATICS OF REDUNDANT MANIPULATORS

We consider a manipulator with n degrees of freedom whose joint variables are denoted by $\mathbf{q} = [q_1, q_2, \dots, q_n]^T$. We assume that a class of tasks we are interested in can be described by m variables, $\mathbf{x} = [x_1, x_2, \dots, x_m]^T$ ($m < n$) and that the relation between \mathbf{q} and \mathbf{x} is given by:

$$\mathbf{x} = f(\mathbf{q}) \quad (1)$$

where f is a function representing the direct kinematics. Differentiating (1) with respect to time yields:

$$\dot{\mathbf{x}} = \mathbf{J}(\mathbf{q})\dot{\mathbf{q}} \quad (2)$$

where $\dot{\mathbf{x}} \in \mathcal{R}^m$, $\dot{\mathbf{q}} \in \mathcal{R}^n$ and $\mathbf{J}(\mathbf{q}) = \partial f(\mathbf{q}) / \partial \mathbf{q} \in \mathcal{R}^{m \times n}$. Hence, it is possible to calculate a path $\mathbf{q}(t)$ in terms of a prescribed trajectory $\mathbf{x}(t)$ in the operational space. We assume that the following condition is satisfied:

$$\max \text{rank} \{ \mathbf{J}(\mathbf{q}) \} = m \quad (3)$$

Failing to satisfy this condition usually means that the selection of manipulation variables is redundant and the number of these variables m can be reduced. When condition (3) is satisfied, we say that the degree of redundancy of the manipulator is $n-m$. If, for some \mathbf{q}

$$\text{rank} \{ \mathbf{J}(\mathbf{q}) \} < m \quad (4)$$

then the manipulator is in a singular state. This state is not desirable because, in this region of the trajectory, the manipulating ability is very limited.

Most of the approaches for solving redundancy that have been proposed [5, 8] are based on the

inversion of equation (2). A solution in terms of the joint velocities, is sought as

$$\dot{q} = K(q)\dot{x} \quad (5)$$

where K is a suitable ($n \times m$) control matrix based on the Jacobian matrix

$$\dot{q} = J^\#(q)\dot{x} \quad (6)$$

where $J^\#$ is one of the generalized inverses of the J [8, 9].

It can be easily shown that a more general solution to equation (2) is given by

$$\dot{q} = J^+(q)\dot{x} + [I - J^+(q)J(q)]\dot{q}_0 \quad (7)$$

where I is the ($n \times n$) identity matrix and $\dot{q}_0 \in \mathbb{R}^n$ is a ($m \times 1$) arbitrary joint velocity vector and J^+ is the pseudoinverse of the J . The solution (7) is composed of two terms. The first term is relative to minimum norm joint velocities. The second term, the *homogeneous solution*, attempts to satisfy the additional constraints specified by \dot{q}_0 .

Moreover, the matrix $I - J^+(q)J(q)$ allows the projection of \dot{q}_0 in the null space of J . A direct consequence is that it is possible to generate internal motions that reconfigure the manipulator structure without changing the gripper position and orientation [7, 9, 10, 11]. Another aspect revealed by the solution of (6) is that repetitive trajectories in the operational space do not lead to periodic trajectories in the joint space. This is an obstacle for the solution of many tasks because the resultant robot configurations have similarities with those of an chaotic system.

III. TRAJECTORY CONTROL OF REDUNDANT AND HYPER-REDUNDANT MANIPULATORS

In this section the formulations developed previously are employed for several redundant manipulators.

The direct kinematics and the Jacobian of a k -link planar manipulator has a simple recursive nature according with the expressions:

$$\begin{bmatrix} x \\ y \end{bmatrix} = \begin{bmatrix} l_1 C_1 + l_2 C_{12} + l_3 C_{123} + \dots + l_k C_{12\dots k} \\ l_1 S_1 + l_2 S_{12} + l_3 S_{123} + \dots + l_k S_{12\dots k} \end{bmatrix} \quad (8.a)$$

$$J = \begin{bmatrix} -l_1 S_1 - l_2 S_{12} - \dots - l_k S_{1\dots k} & \dots & -l_k S_{1\dots k} \\ l_1 C_1 + l_2 C_{12} + \dots + l_k C_{1\dots k} & \dots & l_k C_{1\dots k} \end{bmatrix} \quad (8.b)$$

where l_i is the length of link i , $S_{i\dots k} = \text{Sin}(q_i + \dots + q_k)$ and $C_{i\dots k} = \text{Cos}(q_i + \dots + q_k)$. During the experiments, for all manipulators, it is considered $\Delta t = 0.001 \text{sec}$, $l_1 + l_2 + l_3 \dots + l_k = 3$ and $l_1 = l_2 = l_3 \dots = l_k$

In the closed-loop pseudoinverse's method the joint positions can be computed through the time integration of the velocities according with the block diagram of the inverse kinematics algorithm depicted in Figure 1.

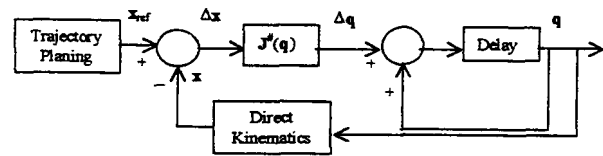


Fig. 1: Block diagram of the closed-loop inverse kinematics algorithm with the pseudoinverse.

The symbolic formulae for the inverse dynamics of a k -link planar manipulator can be also formulated recursively as:

$$\begin{aligned} T = & \sum_{i=1}^n (m_i (\sum_{p=1}^{i-1} (If [j > p, B1 = 0, B1 = 1] l_p^2 \sum_{u=1}^p \ddot{q}_u B1) \\ & + r_i^2 \sum_{u=1}^i \ddot{q}_u + \sum_{p=2}^i (\sum_{k=1}^{p-1} (If [p > i-1, B2 = 0, B2 = 1] \\ & [If [p = i, B3 = 1, B3 = 0]] If [j > k, B4 = 0, B4 = 1] \\ & If [j \geq k+1 \& \& j \leq p), B5 = 1, B5 = 0] \\ & l_k (l_p B2 + r_p B3) ((-\sum_{u=k+1}^p \dot{q}_u)^2 + \\ & 2 \sum_{u=1}^k \dot{q}_u \sum_{u=k+1}^p \dot{q}_u) + C_{k+1\dots p} (\sum_{u=1}^p \dot{q}_u + \sum_{u=1}^k q_u))) B4 + \\ & (S_{k+1\dots p} (\sum_{u=1}^k \dot{q}_u)^2 + C_{k+1\dots p} \sum_{u=1}^k \ddot{q}_u) B5 + \\ & g (\sum_{p=1}^{i-1} (If [j > p, B1 = 0, B1 = 1] l_p C_{1\dots p} B1) + r_i C_{1\dots i}))) \end{aligned} \quad (9)$$

where T are the joints torques, $B1$ to $B5$ are logical conditions, m_i is the mass of link i , r_i is the distance from the joint axis to the link center of mass and g is the acceleration due to gravity.

Based on equation (8) and (9) the next sub-sections we analyze the kinematic and dynamic performances of several planar redundant robots, when subjected to a repetitive circular trajectory in the operational space with radius ρ .

A Kinematics of Redundant Manipulators

In this experiment we adopt the 3R arm with an initial posture $q(0) = [\pi \quad -\pi/2 \quad -\pi/2]^T$. Figure 2 shows the joint positions for the inverse kinematic

algorithm (6) where $\mu = \sqrt{\det(\mathbf{J}\mathbf{J}^T)}$ the index of manipulability.

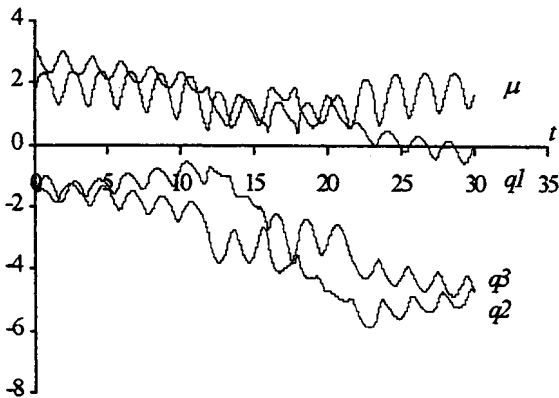


Fig. 2: The 3R-robot joint positions versus time using the pseudoinverse method ($\rho = 0.5$).

Repeating the experiment for the 4R and 5R hyper-redundant robots (Figs. 3 and 4) we observe performances similar to those revealed previously, namely the appearance of non-periodic motions with regions of severe variations that lead to high joint transients [12].

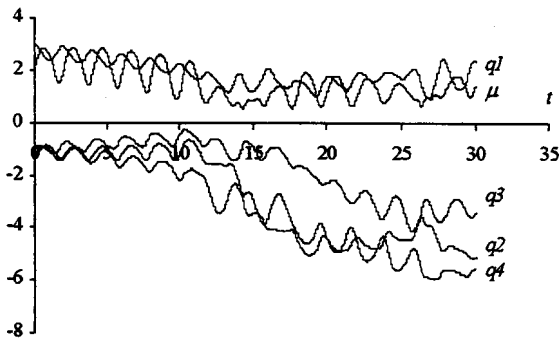


Fig. 3: The 4R-robot joint positions versus time using the pseudoinverse method ($\rho = 0.5$).

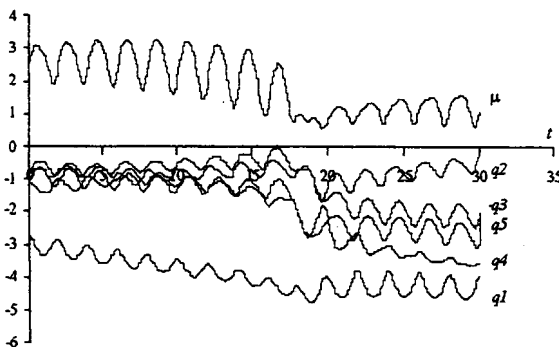


Fig. 4: The 5R-robot joint positions versus time using the pseudoinverse method ($\rho = 0.5$).

B Dynamics of Redundant Manipulators

In a second set of experiments we analyze the robot inverse dynamics when subjected to the repetitive circular trajectory in the operational space. Figure 5 shows the resulting joint torque for the 3R manipulator. It is clear that the dynamics follows the kinematic non-repetitive responses and, therefore, exhibits the same type of problems.

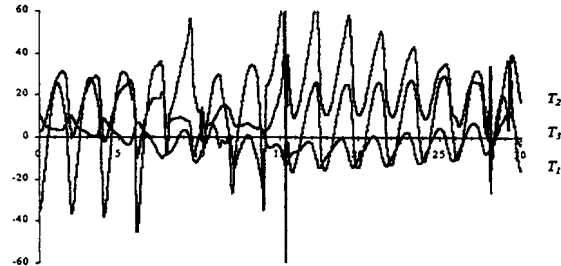


Fig. 5: The 3R-robot joint torque versus time using the pseudoinverse method ($\rho = 0.5$).

IV. ANALYZING THE CHAOTIC-LIKE RESPONSES OF THE PSEUDOINVERSE ALGORITHM

It was shown previously that the pseudoinverse algorithm leads to unpredictable arm configurations, with responses similar to those of a chaotic system [12, 13].

For example, Figures 6-8 and 9-11 depict the phase-plane joint trajectories for the 3R-robot positions and torques, respectively, when repeating a circular motion, with center at $r = 1$ and radius $\rho = 0.1$. Besides the position and velocity drifts, leading to different trajectory loops, we have points that are 'avoided'. Such points correspond to arm configurations where several links are aligned. This characteristic is inherent to the pseudoinverse matrix because the 3R-robot was tested both under open-loop and closed-loop control, leading to the same type of behavior. In order to gain further insight into the pseudoinverse chaotic nature, the robots under investigation were required to follow the cartesian repetitive circular motion for several radial distances (r). The phase-plane joint trajectories were then analyzed and their fractal dimension (dim) estimated through the standard box-counting method:

$$\dim S = \lim_{\epsilon \rightarrow 0} \frac{\ln N(\epsilon)}{\ln(1/\epsilon)} \quad (10)$$

where $N(\epsilon)$ denotes the smallest number of bi-dimensional boxes of side length ϵ required in order to completely cover the plot surface S [13].

Figure 12 shows the resulting chart revealing that:

- for the pseudoinverse method we have $dim \approx 2$ due to the position and velocity drifts, in contrast with the 'standard' case where we have $dim \approx 1$.
- the fractal dimension diminishes near the maximum radial distance (i.e. $r = 3$).
- for each type of robot (3R, 4R and 5R) the fractal dimension is nearly the same, for all joints.

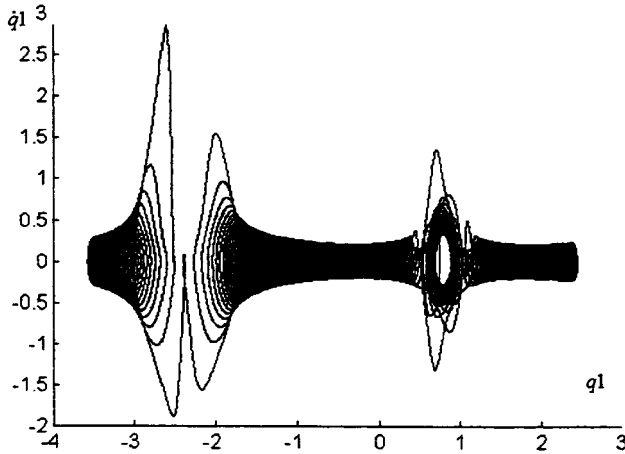


Fig. 6: Phase plane trajectory for the 3R-robot - joint 1 at $r = 1$, $\rho = 0.1$, $dim = 1.62$.

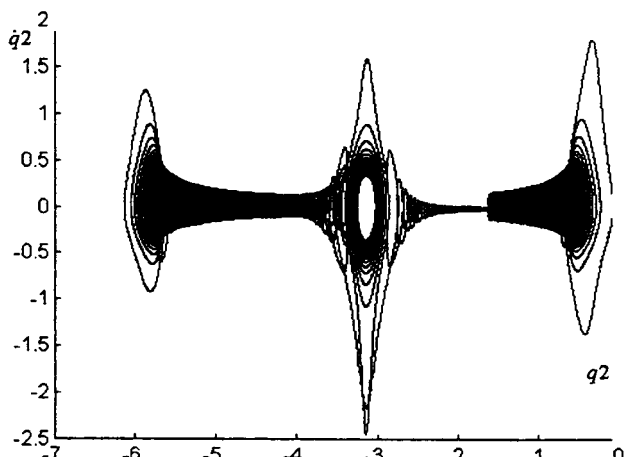


Fig. 7: Phase plane trajectory for the 3R-robot - joint 2 at $r = 1$, $\rho = 0.1$, $dim = 1.60$.

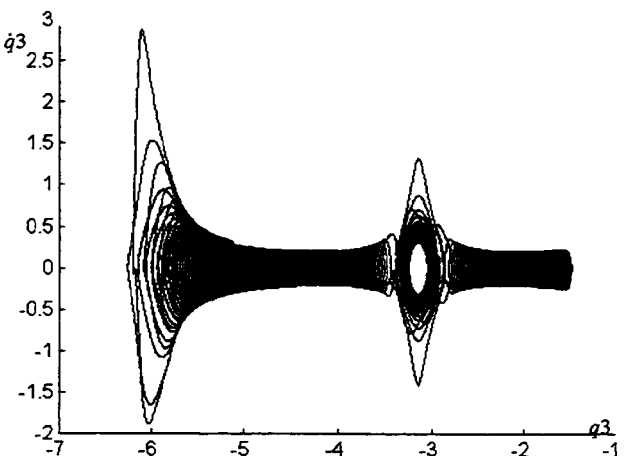


Fig. 8: Phase plane trajectory for the 3R-robot - joint 3 at $r = 1$, $\rho = 0.1$, $dim = 1.63$.

In conclusion, the pseudoinverse method leads to chaotic responses with fast transients. Therefore, in order to overcome those limitations other methods must be envisaged [14, 15].

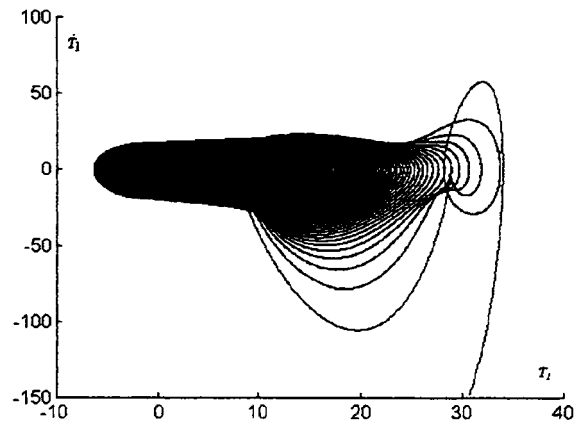


Fig. 9: Phase plane trajectory for the 3R-robot - torque 1 at $r = 1$, $\rho = 0.1$, $dim = 1.69$.

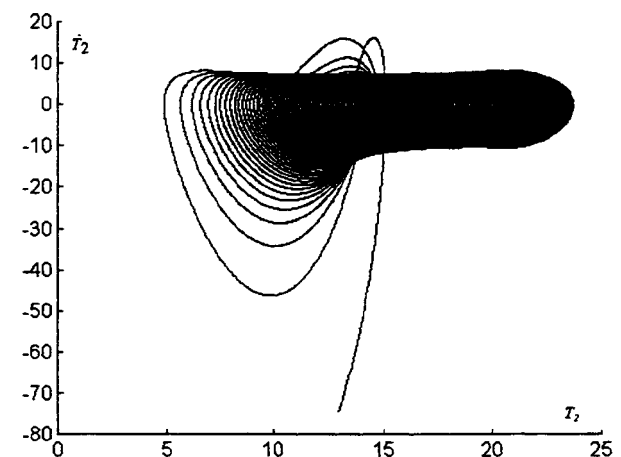


Fig. 10: Phase plane trajectory for the 3R-robot - torque 2 at $r = 1$, $\rho = 0.1$, $dim = 1.70$.

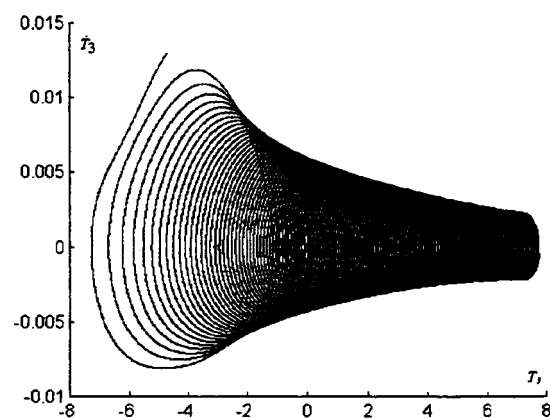


Fig. 11: Phase plane trajectory for the 3R-robot - torque 3 at $r = 1$, $\rho = 0.1$, $dim = 1.71$.

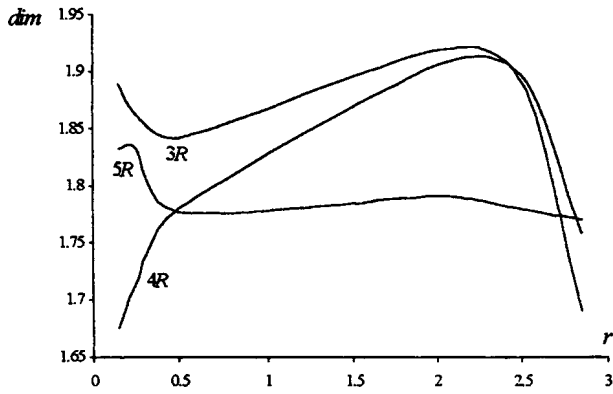


Fig. 12: Fractal dimension of the kinematic phase-plane versus the radial distance for the 3R, 4R and 5R robots, $\rho = 0.1$.

The robot chaotic motion is due to the uncontrolled behavior of the Jacobian pseudoinverse contribution to the manipulator inner motion. Nevertheless, a deeper insight into the nature of this motion must be envisaged. Therefore, two distinct experiments were devised in order to establish the texture of the Jacobian null space.

In a first set of experiments, the robot is required to follow circular motions in the operational space with fixed center but different radius ρ . The resulting charts of the robot joint velocities, over a large number of cycles, is then approximated numerically through a Fourier series.

The constant term for the velocity series approximation is, in fact, the term responsible for the drift in the phase plane charts depicted previously. The results reveal that the amplitude of the velocity drift is 'induced' by the amplitude of the circle radii. The corresponding analytical relationship is of the

type $\dot{q}_i \sim \rho^\alpha$ ($i = 1, 2, 3$) with $\alpha \approx 2.37$ and, therefore, the higher the amplitude of ρ the more serious becomes the robot chaotic response.

In a second experiment, the robot is required to start in an initial random configuration with $q_i \in [-\pi, \pi]$ ($i = 1, 2, 3$) and to attain a fixed point in the operation space under the control of the pseudoinverse scheme. After elapsing the trajectory transient, the final robot joint positions are recorded. The experiment is repeated in order to establish a statistical characterization of the manipulator steady-state configuration. Figure 13 shows a typical histogram for the 3R robot joint positions. For a given desired position in the operational space, we conclude that the possible robot configurations have distinct probabilities. In this perspective, Figure 14 shows the variation of the most probable q_i ($i = 1, 2, 3$) versus the radial distance r ($x = r$ and $y = 0$).

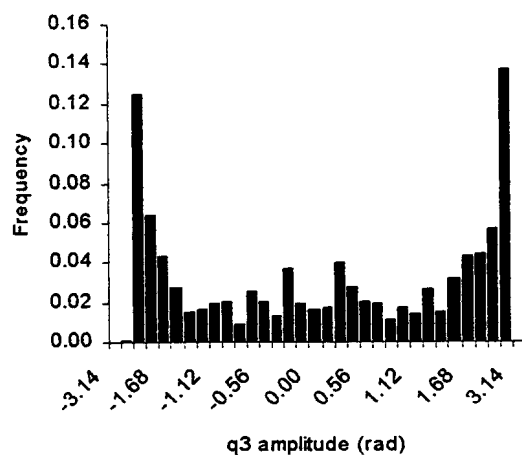
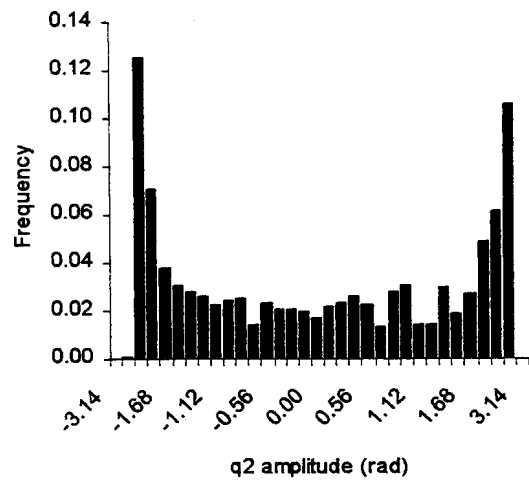
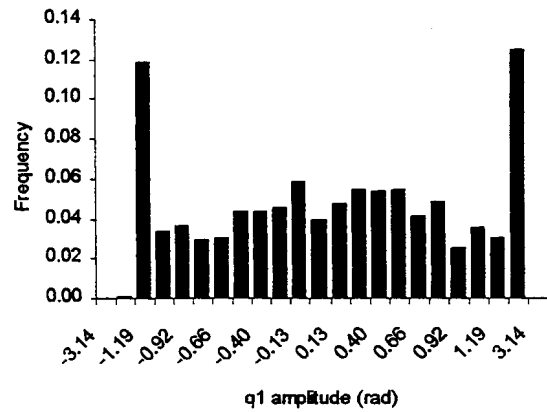


Fig. 13: Histogram for the 3R robot joint positions, $(x, y) = (\sqrt{2}, \sqrt{2})$.

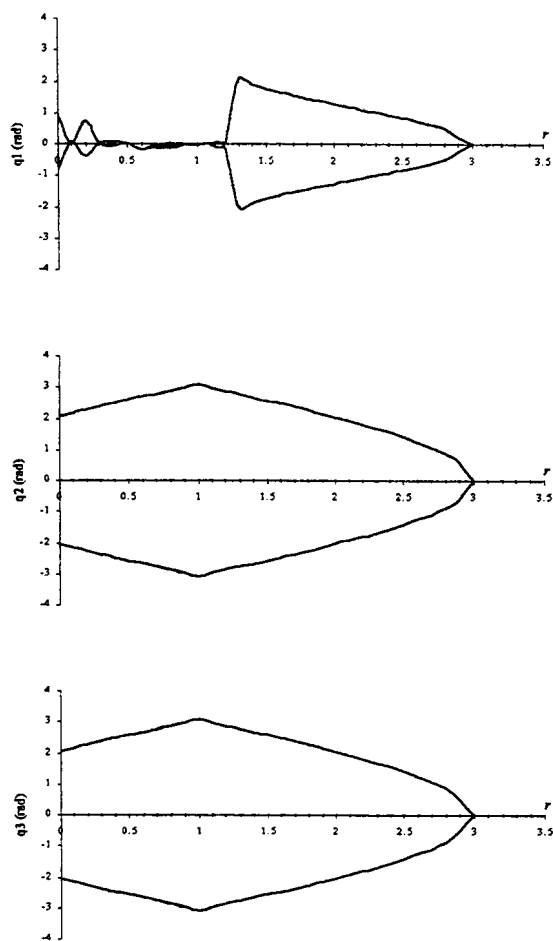


Fig. 14: Most probable robot joint positions versus the radial distance r .

V. CONCLUSIONS

This paper discussed several aspects of the chaotic phenomena generated by the pseudoinverse-based trajectory control of redundant manipulators. Furthermore, the study addressed both the kinematics and dynamics in order to test the influence of each model. In this perspective, the fractal dimension of the responses was analyzed showing that it is independent of the robot joint. In fact, the chaotic motion depends solely on the operational space point and on the amplitude of the exciting repetitive motion. Moreover, a second group of experiments reveals that the robot inner motion, that spans the null space of the Jacobian matrix, leads to 'preferred' configurations while avoiding other areas. Nevertheless, the relationship between the fractal dimension of the phase plane portraits, the amplitude of the exciting repetitive signal and the statistics of the robot joint configurations is not completely clear and further research on this aspects needs still to be done in order to develop superior trajectory planning algorithms.

VI. REFERENCES

- [1] E. Sahin Conkur, and Rob Buckingham "Clarifying the Definition of Redundancy as Used in Robotics", *Robotica*, vol. 15, pp. 583-586, 1997.
- [2] S. Chiaverini "Singularity-Robust Task-Priority Redundancy Resolution for Real Time Kinematic Control of Robot Manipulators", *IEEE Trans. Robotics Automation*, vol. 13, pp. 398-410, 1997.
- [3] C.A Klein, and C. C Huang, "Review of Pseudoinverse Control for Use With Kinematically Redundant Manipulators", *IEEE Trans. Syst. Man, Cyber.*, vol. 13, pp. 245-250, 1983.
- [4] Yoshikawa, T., "Foundations of Robotics: Analysis and Control", MIT Press, 1988.
- [5] Rodney Roberts R. and Anthony Maciejewski, "Singularities, Stable Surfaces and Repeatable Behavior of Kinematically Redundant manipulators", *International Journal of Robotics Research*, vol. 13, pp. 70-81, 1994.
- [6] John Bay, "Geometryn and Prediction of Drift-free trajectories for Redundant Machines Under Pseudoinverse Control", *International Journal of Robotics Research*, vol. 11, pp. 41-52, 1992.
- [7] Y. Nakamura, "Advanced Robotics: Redundancy and Optimization", Addison-Wesley, 1991.
- [8] Keith L. Doty, C. Melchiorri and C. Bonivento, "A Theory of Generalized Inverses Applied to Robotics", *International Journal of Robotics Research*, vol. 12, pp. 1-19, 1993.
- [9] Bruno Siciliano, "Kinematic Control of Redundant Robot Manipulators: A Tutorial", *Journal of Intelligent and Robotic Systems*, vol. 3, pp. 201-212, 1990.
- [10] W.J.Chung, Y. Youm and W. K. Chung, "Inverse Kinematics of Planar Redundant Manipulators via Virtual Links With Configuration Index", *J. of Robotic Systems*, vol. 11, pp. 117-128, 1994.
- [11] Sanjeev Seereeram and John T. Wen, "A Global Approach to Path Planning for Redundant Manipulators", *IEEE Trans. Robotics Automation*, vol. 11, pp.152-159, 1995.
- [12] Fernando B.M. Duarte and J.A. Tenreiro Machado, "Kinematic Optimazition of Redundant and Hyper-Redundant Robot Trajectories", ICECS'98-5th IEEE International Conference on Electronics, Circuits and Systems, Lisbon, Portugal, 1998.
- [13] James Theiler, "Estimating Fractal Dimension", *Journal Optical Society of America*, vol. 7, n^o6, pp. 1055-1073, 1990.
- [14] J.A.Tenreiro Machado and Fernando B. Duarte, "Redundancy Optimization for Mechanical Manipulators", *AMC'98-5th IEEE Int. Workshop on Advanced Motion Control*, Portugal, 1998.
- [15] Fernando B. Duarte and J.A. Tenreiro Machado, "On the Optimal Configuration of Redundant Manipulators", INES'98- 9th IEEE Int. Conf. on Intelligent Engineering Systems, Vienna, Austria, 1998.